

Porous Multilayered Films Based on poly(3,4-ethylenedioxythiophene) and poly(indole-5-carboxylic acid) and Their Capacitance Performance

Danqin Li¹, Danhua Zhu², Weiqiang Zhou^{3,*}, Xiumei Ma², Qianjie Zhou², Guo Ye¹, Jingkun Xu^{1,*}

¹ School of Pharmacy, Jiangxi Science and Technology Normal University, Nanchang 330013, China

² Jiangxi Key Laboratory of Organic Chemistry, Jiangxi Science and Technology Normal University, Nanchang 330013, China

³ Jiangxi Engineering Laboratory of Waterborne Coatings, Jiangxi Science and Technology Normal University, Nanchang 330013, China

*E-mail: zhouwqh@163.com, xujingkun@jxstnu.edu.cn

Received: 10 January 2017 / Accepted: 23 February 2017 / Published: 12 March 2017

Layer-by-layer (LBL) technique is a prevalent way to construct multilayered films. Herein, using high conducting poly(3,4-ethylenedioxythiophene) (PEDOT) and good stable redox-active poly(indole-5-carboxylic acid) (5-PICA), an alternately multilayered porous films has been prepared by the electrochemical LBL method. The alternately multilayered films were characterized by scanning electron microscope (SEM), cyclic voltammetry (CV), galvanostatic charge-discharge (CD) and electrochemical impedance spectroscopy (EIS) techniques. Compared with monolayered PEDOT (147.8 F g⁻¹) and 5-PICA(198.3 F g⁻¹), the PEDOT/5-PICA/PEDOT/5-PICA 4-layered film exhibited a higher specific capacitance which reached 281.7 F g⁻¹ at 20 A g⁻¹ in 1.0 M H₂SO₄ solution. Furthermore, the specific capacitance of 4-layered film still had good stability, viz., 73% retention after 1000 cycles at the range of potential -0.15 to 1.0 V and even reached 95% if the potential range was from -0.15 to 0.8 V. Therefore, these results indicated that the PEDOT/5-PICA/PEDOT/5-PICA was a potential electrode material for supercapacitors.

Keywords: Conducting polymers; Electropolymerization; Layer-by-layer films; Specific capacitance

1. INTRODUCTION

As the energy storage devices, supercapacitors have been considered as the most promising candidates, which have been widely applied by digital telecommunication systems and hybrid electric vehicles due to their long cycle life, superior power density, and fast charge/discharge capability [1-6].

Depending on the energy storage mechanism, supercapacitors could be divided as the electrical double-layer capacitors (EDLCs) and the pseudocapacitors (redox supercapacitors) [3,7-9]. Generally, the former possess much lower specific capacitance than the latter. And the pseudocapacitors rely on surface fast and reversible redox reactions to store energy, which was 10-100 times higher than that of electrical double-layer capacitors [10]. As a result, it has been used to build supercapacitor with improved energy and power densities. Conducting polymers and metal oxides were used for redox materials [10-12].

To obtain high-performance supercapacitors, the electrolyte selection, the preparation of active materials, and the architecture of the device all are vital. Among these factors, there have been many studies on the choice and preparation of active materials such as carbon nanotubes, reduced graphene oxide, nanostructural manganese dioxide and nanostructural conducting polymers. The layered structural materials have been proved that they have better electrochemical behaviors and higher ability to store charge than that of the individual material [13-18]. Currently, above mentioned materials are used to build the alternately layered composite films by the LBL assembly technique, which showed high capacitive behaviors. For instance, Shin *et al.* prepared $(\text{NH}_2\text{-MWCNT/OA-Fe}_3\text{O}_4\text{-MWCNT})_{20}$ and $(\text{NH}_2\text{-MWCNT/OA-MnO-MWCNT})_{20}$, their volumetric capacitances reached approximately 394 and 674 F cm^{-3} at 1 A cm^{-3} [16]. Tang *et al.* fabricated different PEDOT/MnO₂/PEDOT sandwich electrodes that possesses a specific capacitance of 179-288 F g^{-1} at 1 A g^{-1} [14]. Sarker *et al.* built the multilayer films composed of reduced graphene oxide/polyaniline bilayers, and as-prepared $(\text{PANi/RGO})_{15}$ showed a volumetric capacitance of 584 F cm^{-3} at 3.0 A cm^{-3} [19]. Aradilla *et al.* fabricated 3-layered PEDOT/PPy/PEDOT films on steel uncoated and coated with octanethiol, which showed the specific capacitance of 101-164 F g^{-1} [20]. The integration of different materials by a LBL stacking method is beneficial for the formation of an intimate interface for charge transport, generating a synergistic effect. [17]. Thus the synergistic effect mainly appeared the interface between the bilayers can promote the enhancement of electrochemical stability and activity [21].

Compared with carbon-based materials, conducting polymers (CPs) such as polyaniline (PANi), polypyrrole (PPy) and polythiophene (PTh) have higher theoretical specific capacitance and higher energy density. However, these typical CPs showed low cycle stability, which forces researchers to explore novel materials that combine high specific capacitance and long cycle life. As PTh derivative, PEDOT is one kind of good conductive polymer due to its high conductivity up to 500 S cm^{-1} [22] and higher stability than other conductive polymers [23]. Yet the specific capacitance of PEDOT is lower ($120 \pm 40 \text{ F g}^{-1}$) [24-27], which is only comparable with that of carbon-based materials. Additionally, similarly to PANi and PPy, poly(indole-5-carboxylic acid) (5-PICA) nanowires was found to have high specific capacitance and long cycle stability [3,4]. However, the low conductivity of 5-PICA, about $3 \times 10^{-3} \text{ S cm}^{-1}$ [28] greatly hindered the charge transfer in thick film. For the aim about seeking high-performance capacitive materials, the novel materials formed by combination of PEDOT with 5-PICA are worth studying.

In light of aforementioned many advantages about multilayered composite films, to construct alternately multilayered films based on PEDOT and 5-PICA will overcome their weaknesses, thus helping to obtain the composite materials with higher capacitance performance. Herein, by

electrochemical LBL method, we have successfully prepared the alternately multilayered porous PEDOT/5-PICA films. The layered structures, surface morphologies and capacitance properties of multilayered PEDOT/5-PICA were clearly characterized. It is found that the multilayered film showed an enhanced capacitance behaviors compared with those of individual PEDOT and 5-PICA.

2. MATERIALS AND METHODS

2.1. Materials

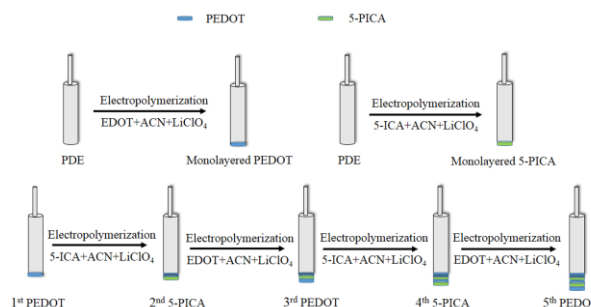
3,4-Ethylenedioxythiophene (EDOT) monomer was purchased from Energy Chemical (Shanghai, China) and purified by distilled under reduced pressure before use. Indole-5-carboxylic acid (5-ICA) was purchased from Shanghai Vita Chemical Reagent Co., Ltd. China. Acetonitrile (ACN) was supplied by Shanghai Lingfeng Chemical Reagent Co., Ltd. Lithium perchlorate (LiClO_4) was purchased from Xiya Reagent Research Center. Deionized water and anhydrous ethanol were used throughout the work. All the other chemical reagents were used as received in analytical grade.

2.2. Apparatus

The electrochemical experiments were measured on CHI660E (Chenhua, Shanghai, China) electrochemical working station. Platinum disk electrode (PDE) (3 mm diameter, 0.07 cm^2 surface area) as the substrate electrode was purchased from Gaoss Union (Wuhan) Technology Co., Ltd. China. The counter electrode was platinum wire (1 mm diameter). Ag/AgCl electrode and saturated calomel electrode (SCE) were used for reference electrode, respectively. Notice that the Ag/AgCl electrode was used for the preparation of polymer films while the SCE was used for the capacitance test of the multilayered films. SEM measurements were carried out by using scanning electron microscope (JSM-5600, JEOL).

2.3. Preparation of multilayered films

As shown in scheme 1, the monolayered PEDOT was obtained by electropolymerization in 5 mL ACN solution containing 0.1 M LiClO_4 and a certain amount of EDOT monomer. The preparation of monolayered 5-PICA adopted the same method in 5 mL ACN solution containing 0.1 M LiClO_4 and a certain amount of 5-ICA monomer. The multilayer films was prepared by the electrochemical LBL technique. Initially, a thin layer of PEDOT as the first layer was potentiostatically prepared on PED electrode. Next, 5-PICA film as the second layer was potentiostatically deposited on the PEDOT/PED, forming 5-PICA/PEDOT/PED electrode. According to above sequence, the alternately multilayered films based on PEDOT and 5-PICA were prepared. The mass of each layer was controlled by the total charge passed through the cell during the polymer film growth process. Notice that each electrode mentioned in the text has the same charge.



Scheme 1. Schematic diagrams of the electrochemical deposition of monolayered PEDOT, monolayered 5-PICA and 5-layered composite film.

The mass of monolayered polymer film (W_p) can be calculated by equation (1) [3]:

$$W_p = (\eta Q_{dep})(M)/F Z \quad (1)$$

Above of the formula, η is stand for current efficiency, which has been assumed to 100%. Q_{dep} is the total charge passed through the cell during the polymer film growth process. M is the molecular weight of monomer (EDOT, 5-ICA), F is the Faraday constant (96485 C mol^{-1}), Z is the number of electrons transferred per monomer attached to the polymer, in which $Z = 2 + f$. f is called the doping level. Here, the doping level of PEDOT and 5-PICA is 0.3 and 0.23, respectively, assuming a 100% current efficiency, according to equation (2) [11]:

$$f = 2Q_0/(Q_d - Q_0) \quad (2)$$

Where Q_d is the total charge used for polymer film growth process, and Q_0 is the total charge of oxidized species in the polymer films.

2.4. Capacitance calculation

Specific capacitance (C) of the multilayered films was calculated from CV curve by means of equation (3) [29]:

$$C = \int_{E_2}^{E_1} i(E)d(E)/2vm(E_2 - E_1) \quad (3)$$

where E_1 and E_2 are the cutoff potentials in cyclic voltammetry, $i(E)$ is the instantaneous current, $\int_{E_2}^{E_1} i(E)d(E)$ is the total voltammetric charge obtained by integration of the positive and negative sweeps in the cyclic voltammograms, v is the scan rate, and m is the mass of the sample on electrode.

The specific capacitances were also obtained according to the equation (4) if used the charge-discharge method [30]:

$$C = I\Delta t/m\Delta V \quad (4)$$

where C is specific capacitance (F g^{-1}), I is the charge-discharge current, Δt is the discharge time, ΔV is the potential window during the discharge process, and m is the mass of sample on PED.

The energy density (E , Wh kg⁻¹) and power density (P , W kg⁻¹) values were calculated by the following relationships: [31]

$$E = 1/2 C \Delta V^2 \quad (5)$$

$$P = E/\Delta t \quad (6)$$

Here, C is the specific capacitance, ΔV is the voltage window, and Δt is the discharge time.

3. RESULTS AND DISCUSSION

3.1. Chronoamperogram of film electrodeposition

Fig. 1 shows the chronoamperogram of each stage during the preparation of 5-layered film and monolayered 5-PICA. For the electrodeposition of each layer, the applied potential for PEDOT and 5-PICA is 1.4 V and 1.1 V, respectively. In Fig. 1, the current increases gradually with the increase in the number of layer. This indicated that the specific surface area and/or conductivity of film increase. However, after the third layer, the increased degree of current obviously decreases. This is possibly because the resistance of film increases when the thickness of film increases, especially, the introduced 5-PICA with low conductivity.

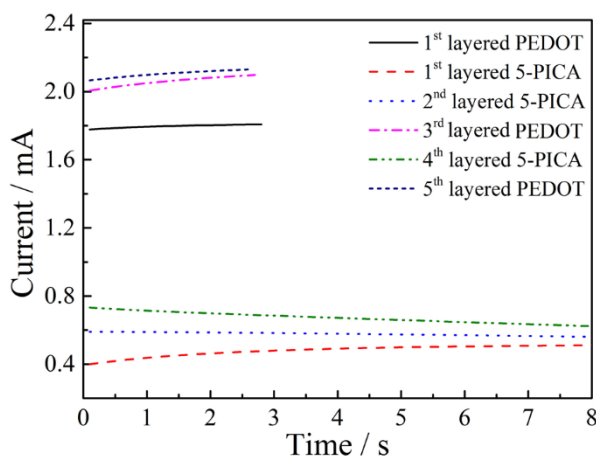


Figure 1. Chronoamperogram of each stage during the preparation of 5-layered film and monolayered 5-PICA.

3.2. Morphology

The surface morphologies of the different layered films were studied by means of SEM, as shown in Fig. 2. Distinctly, PEDOT has relative compact surface while 5-PICA shows a porous surface being composed of clear nano-wires. With increase in the number of layer, the porous surface was more obvious and the pore diameter was larger. From the cross-section of trilayer film, the interlayer of sandwich structural film shows porous structure. This implies that the introduction of 5-PICA facilitates the formation of the multilayered porous films. As a supercapacitor material, these

multilayered films possessing porous structure will have following advantages: (1) the micro/nano-sized pores provide a high interfacial reaction area and promote the ions adsorption and desorption at the electrode/electrolyte interface; (2) It can significantly accelerate the intercalation of ions and enhance the utilization rate of electrode material due to the efficient diffusion paths for electrolyte ions created by the porous network of 5-PICA; (3) PEDOT layers with high conductivity can accelerate electronic transmission in multilayered films.

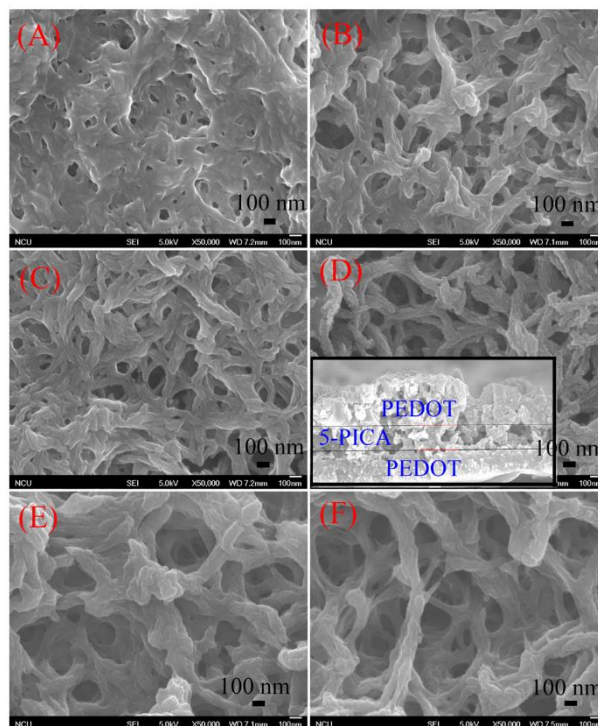


Figure 2. SEM images of monolayered PEDOT (A), monolayered 5-PICA (B), 2-layered film (C), 3-layered film (D), 4-layered film (E), 5-layered film (F). Inset in (D) shows the cross-section SEM of 3-layered film.

3.3. Electrochemical properties of multilayered films

In order to get the optimal electrodeposition conditions of PEDOT and 5-PICA nano-wires in the following work, the monomer concentrations and deposition potentials were optimized, as demonstrated in Fig. 3 (A-C). The result indicates that specific capacitance of monolayered PEDOT and monolayered 5-PICA nano-wires reached maximum values when the concentrations of EDOT and 5-ICA were 120 mM and 50 mM, respectively. When the electrodeposition potentials of PEDOT and 5-PICA were 1.4 V and 1.1 V, respectively, they also got maximum values. What is noteworthy is that the power of (A), (B) and (C) were all 20 mC. Therefore, in order to investigate the influence of PEDOT/5-PICA electricity ratio and be easy to calculate, there selected 30 mC for next following work. Fig. 4(A) is the optimization of PEDOT/5-PICA electricity ratio in bilayer film. When PEDOT/5-PICA electricity ratio = 1:5, we can obtain the maximum capacitance 250.4 F g^{-1} .

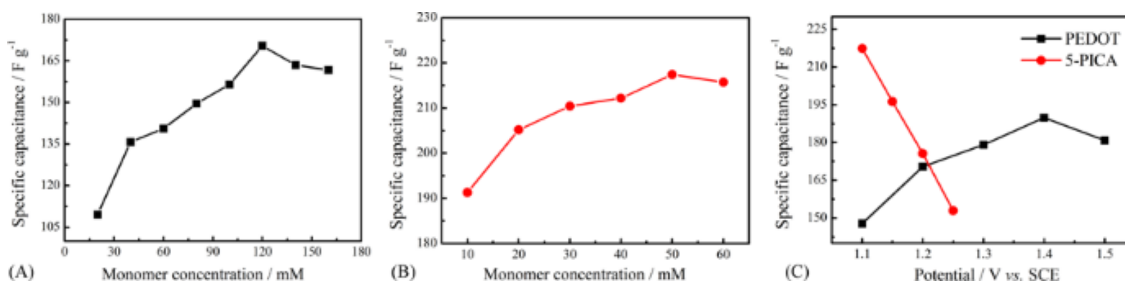


Figure 3. Specific capacitance of PEDOT and 5-PICA as a function of different monomer concentration (A) and (B), respectively, and electrodeposition potential (C). Note that the power of each electrode in (A), (B) and (C) is 20 mC.

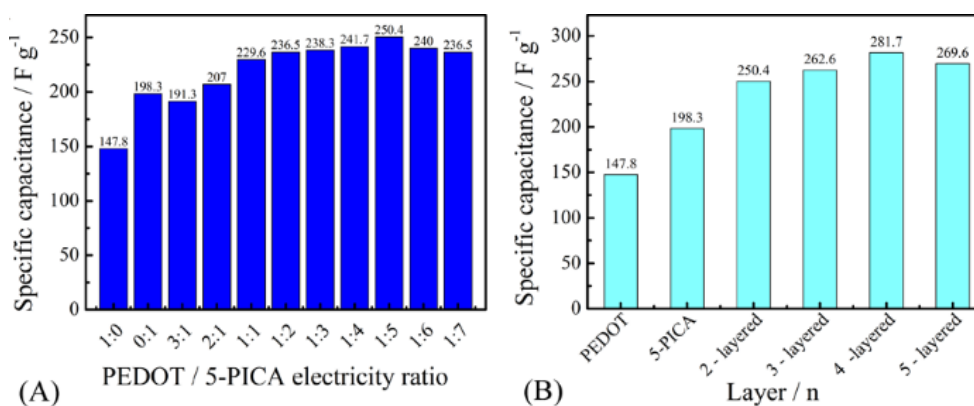


Figure 4. Specific capacitance of 2-layered film PEDOT/5-PICA as a function of PEDOT/5-PICA electricity ratio (A) and specific capacitance of different electrodes (B).in 1 M H₂SO₄ solution at 20 A g⁻¹.

Table 1. Capacitance performance comparison of PEDOT/5-PICA/PEDOT/5-PICA composite film with several similar materials.

Electrode	Test condition	Potential/V	Electrolytes	Capacitance/F g ⁻¹	Ref
ml-PEDOT/PNMPy	100 mV s ⁻¹	2.1	0.1 M LiClO ₄	50 ^{b,2}	13
ml-PEDOT/PNMPy				62 ^{d,2}	
PEDOT/PPy/PEDOT	100 mV s ⁻¹	2.1	0.1 M LiClO ₄	101-150 ^{b,2}	20
PEDOT/c-PPy	2 mV s ⁻¹	1	1 M LiClO ₄	160 ^{a,1}	32
PEDOT/h-PPy			1 M KCl	230 ^{a,1}	
PEDOT/PBEDOT-BT/PEDOT	100 mV s ⁻¹	2.1	0.1 M Bu ₄ NPF ₆	178 ^{b,1}	33
PANI-PPY	6 mA cm ⁻²	1	0.5 M H ₂ SO ₄	523 ^{a,1}	34
PEDOT/5-PICA	20 A g ⁻¹	1.15	1 M H ₂ SO ₄	250.4 ^{a,1}	This work
PEDOT/5-PICA	20 A g ⁻¹	1.15	1 M H ₂ SO ₄	281.7 ^{c,1}	This work

^a Two-layered, ^b three-layered, ^c five-layered, ^d five-layered.

¹ Three-electrode system, ² two-electrode system.

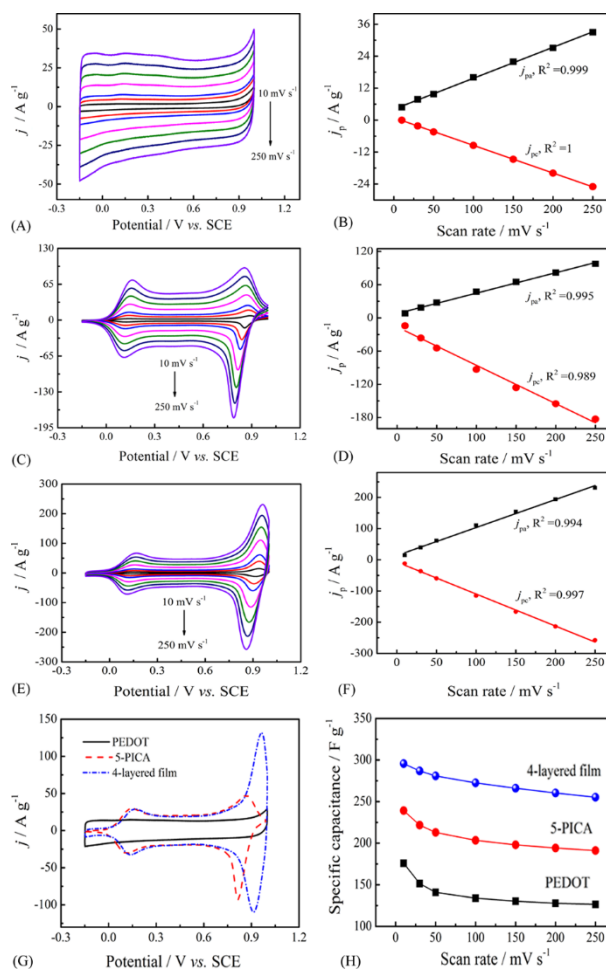


Figure 5. Cyclic voltammograms of PEDOT (A), 5-PICA (C), and 4-layered film (E) electrodes in 1 M H₂SO₄ at potential scan rates of 10, 30, 50, 100, 150, 200, and 250 mV s⁻¹ (*j* = current density). Peak current densities of PEDOT (B), 5-PICA (D) and 4-layered film (F) electrodes as a function of scan rates. Cyclic voltammograms (G) of monolayered PEDOT, 5-PICA and 4-layered films in 1.0 M H₂SO₄ solution at scanning rate of 100 mV s⁻¹ (*j* = current density) and (H) specific capacitance of films as a function of scan rate.

Fig. 4(B) show that the 4-layered PEDOT/5-PICA/PEDOT/5-PICA electrode demonstrated the highest specific capacitance 281.7 F g⁻¹ at 20A g⁻¹. These results were compared with similar materials for capacitors (Table 1), which showed that the specific capacitance of 4-layered electrode was higher than most of reported values of similar material.

Fig. 5(A&C&E) shows the CVs of monolayered PEDOT, 5-PICA and 4-layered films in 1.0 M H₂SO₄ solution at various scan rates of 10, 30, 50, 100, 150, 200, and 250 mV s⁻¹. As it shown, with the increase of scanning rates, there is an increase in the current and no change in the shape of CVs, which indicate it has a good high-rate performance. Specifically, the CV curves of PEDOT film exhibits near rectangular enantiomorphous profiles, which is similar to that of carbon materials; the CV curves of 5-PICA shows two redox peaks at about 0.15 V and 0.8 V, in well agreement with our works [3] and the CV curves of 4-layered film includes the electrochemical properties of both monolayered films and has larger current density. Additionally, the relationship between the peak

current densities and scan rates, as displayed in Fig. 5(B&D&F). As seen from it, the peak current densities were linearly proportional to scan rates, which means the electrochemical behaviors of these electrodes were adsorption controlled process [35]. Namely, these are typical capacitive behaviours or pseudocapacitive behaviours. In Fig. 5(H), at 10 mV s^{-1} , the 4-layered film showed a specific capacitance of 295.7 F g^{-1} , the value is approximately 1.7 times that of PEDOT (175.9 F g^{-1}) and about 1.2 times that of 5-PICA (239.1 F g^{-1}). At 250 mV s^{-1} , the specific capacitance of 4-layered film still reached 255.3 F g^{-1} .

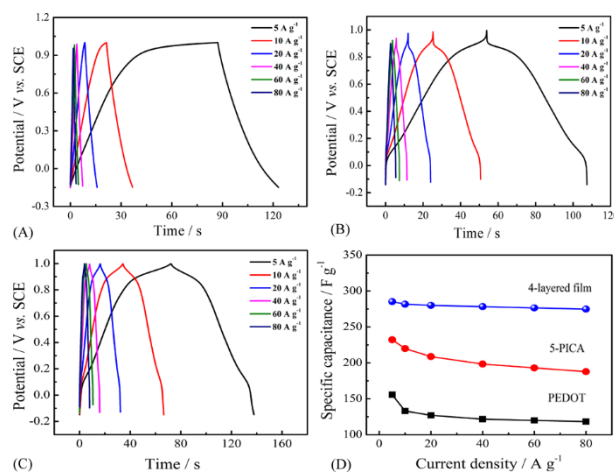


Figure 6. Galvanostatic charge-discharge curves of monolayered PEDOT (A), 5-PICA (B), and 4-layered film (C) at different current densities, and specific capacitances of three electrodes as a function of current densities (D).

Fig. 6 shows the galvanostatic charge-discharge curves of monolayered PEDOT, 5-PICA, 4-layered film at different current densities, and their specific capacitances as a function of current densities. As seen from Fig. 6(A), there is no IR drop at both ends of potential window of CV for monolayered PEDOT films, this is due to the high conducting PEDOT has fast charge transfer ability in the potential window. For 5-PICA, larger IR drop obviously presents than 4-layered film, reflecting that the internal resistance of it is much higher [31]. This result may indicate that the introduction of PEDOT to 5-PICA enhances the charge transport at the intimate interface, thus reducing the IR drop. In Fig. 6(D), at 5 A g^{-1} , the specific capacitances of monolayered PEDOT, 5-PICA, and 4-layered films were 155.7 F g^{-1} , 232.2 F g^{-1} and 285.2 F g^{-1} , respectively. When the current density increased to 20 A g^{-1} , the corresponding specific capacitances were 127.0 F g^{-1} , 208.7 F g^{-1} and 281.7 F g^{-1} , respectively, the total loss was 18.4% for monolayered PEDOT, 10.1% for monolayered 5-PICA and 1.2% for 4-layered film. This implies that the rate capability of the 4-layered film is significantly improved. In addition, the specific capacitance of 4-layered film is about 1.7 times as high as the average value [$(127.0 + 208.7)/2 = 167.9 \text{ F g}^{-1}$] of monolayered PEDOT and 5-PICA, indicating the synergic effect produced between the bilayers, that is, the interface conductivity is enhanced by PEDOT and the porous structure is formed by 5-PICA nano-wires.

The relationship between energy density and power density were depicted in Fig.7. It was observed from Fig. 7, the energy density of the electrode decreases with increasing charge-discharge current. From the 4-layered film, an energy density of 52.4 Wh kg^{-1} is obtained at a specific power of 2.9 kW kg^{-1} . Even at a high specific power of 46.0 kW kg^{-1} , the energy density still retain approximately 50.5 Wh kg^{-1} . Meanwhile, the values are higher than those of monolayered PEDOT and monolayered 5-PICA electrode. In conclusion, the 4-layered electrode material may become a promising material for applications in the field of electrochemical energy storage, which can operate with high power density and high energy density at high rates [36].

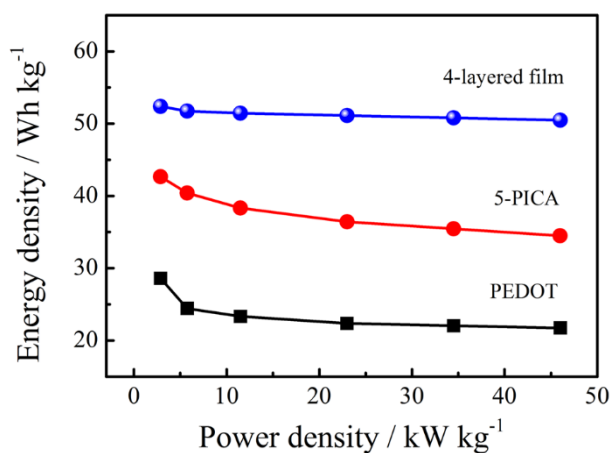


Figure 7. Ragone plots of PEDOT, 5-PICA and 4-layered film electrodes.

To further explore the capacitance performance of 4-layered film electrode, the EIS was studied at 0.8 V in 1 M H_2SO_4 aqueous solution. Fig. 8 shows the impedance spectra of monolayered PEDOT, 5-PICA and 4-layered films. As seen from Fig. 8(A), compared with PEDOT and 4-layered electrode, 5-PICA electrode show a bigger semicircle in high-frequency region, however, PEDOT and 4-layered electrode showed a flattened semicircle at the high-frequency region. These means 5-PICA electrode have a relatively higher the charge-transfer resistance. Besides, 5-PICA and 4-layered electrode exhibit an ideal capacitive behavior of the supercapacitor owing to nearly vertical straight line at the low frequency region. The Bode-magnitude plot was plotted in Fig. 8(B), demonstrating the result was in good agreement with about a capacitive porous nano-wires composite material, because the absolute value of imaginary impedance of three kinds of polymer electrodes at high frequency region were almost independent of frequency. In the phase angle plot (Fig. 8C), the maximum phase angle of PEDOT reached -86.5° at 0.32 Hz, 5-PICA reached -87.9° at 0.01 Hz and PEDOT/5-PICA/PEDOT reached -86.5° at 0.12 Hz. Additionally, according to $C = -1/(2\pi f Z_{im})$, the specific capacitance also can be calculated by the values of the imaginary impedance (Z_{im}). As seen from Fig. 8D, 4-layered PEDOT/5-PICA/PEDOT/5-PICA possessed the maximal capacitance. Above all of the results also display that the 4-layered film may be a promising candidate material for supercapacitor.

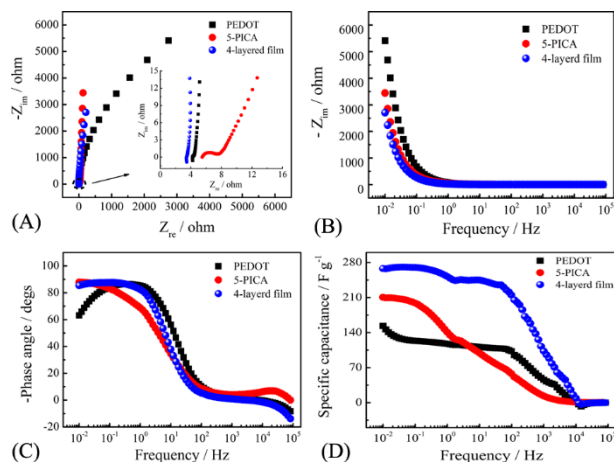


Figure 8. EIS of monolayered PEDOT, 5-PICA films and 4-layered film: (A) Nyquist plots, (B) Bode-magnitude plots, (C) Bode-phase angle plots, (D) Specific capacitance frequency plots of different electrodes.

For the practical application of supercapacitors, the cycling stability is a very important parameter. To research cycling performance of the 4-layered film electrode, the galvanostatic charge-discharge was carried out at 20 A g^{-1} for 1000 cycles (Fig. 9). It can be seen from Fig. 9, in the range of $-0.15\text{-}1.0 \text{ V}$, the monolayered 5-PICA electrode showed an excellent cycling stability with 97% of the initial capacitance at 20 A g^{-1} after 1000 cycles.

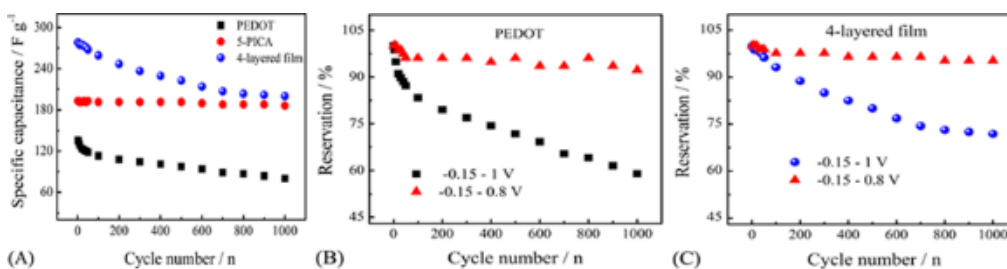


Figure 9. Galvanostatic charge-discharge life of monolayered PEDOT, 5-PICA films and 4-layered film in $1.0 \text{ M H}_2\text{SO}_4$ solution at 20 A g^{-1} .

Monolayered PEDOT electrode only showed the capacitance retention of 59%. This is due to the instability of PEDOT in acidic aqueous solution as applied potential higher than about 0.8 V . However, the capacitance retention of 4-layered film electrode was enhanced compared with monolayered PEDOT film, reaching up to 73%. Fig. 9(B) exhibits that by decreasing the potential of 1.0 V to 0.8 V , the capacitance retention of PEDOT electrode was enhanced to 92% and the capacitance retention of 4-layered film electrode was enhanced to 95%. Therefore, when the potential is controlled to about below 0.8 V , the 4-layered film electrode exhibited excellent cycling stability.

4. CONCLUSIONS

In this paper, a facile electrochemical LBL technique was employed to fabricate alternately multilayered porous films based on high conducting PEDOT and good stable redox-active 5-PICA nano-wires. As-prepared multilayered film verified by cross-sectional SEM was composed of compact PEDOT layer and porous 5-PICA layer. The electrochemical results indicated that 4-layered PEDOT/5-PICA/PEDOT/5-PICA film in 1 M H₂SO₄ solution exhibits a higher specific capacitances of 281.7 F g⁻¹ at 20 A g⁻¹ in comparison with monolayers and other multilayers. In addition, the 4-layered film still showed high specific capacitance of 274.8 F g⁻¹ at 80 A g⁻¹. Moreover, the 4-layered film had an enhanced cycle stability relative to monolayered PEDOT due to the introduction of high stable 5-PICA. Therefore, these intriguing features make the novel 4-layered PEDOT/5-PICA/PEDOT/5-PICA to be a promising electrode material for supercapacitors.

ACKNOWLEDGEMENTS

This work was supported by the National Natural Science Foundation of China (Grant Nos. 51572117, 51662012), the Natural Science Foundation of Jiangxi Province (20161BAB206147), Scientific Research Projects (2016QNBjRC001, 2015CXTD001, YC2016-X14) of Jiangxi Science and Technology Normal University.

References

1. S. Fajardo, D.M. Bastidas, M. Ryan, M. Criado, D. McPhail, R.J. Morris and J. Bastidas, *Appl. Surf. Sci.*, 288 (2014) 423.
2. D. Gopi, P. Karthikeyan, L. Kavitha and M. Surendiran, *Appl. Surf. Sci.*, 357 (2015) 122.
3. X. M. Ma, W. Q. Zhou, D. Z. Mo, Z. P. Wang and J. K. Xu, *Synth. Met.*, 203 (2015) 98.
4. X. M. Ma, W. Q. Zhou, D. Z. Mo, J. Hou and J. Xu, *Electrochim. Acta*, 176 (2015) 1302.
5. P. Sharma and T. Bhatti, *Energy Conversion and Management*, 51 (2010) 2901.
6. J. G. Wang, Y. Yang, Z. H. Huang and F. Y. Kang, *J. Power Sources*, 204 (2012) 236.
7. M. Zabihinpour and H. Ghenaatian, *Synth. Met.*, 175 (2013) 62.
8. X. B. Liu, N. Wen, X. L. Wang and Y. Y. Zheng, *Nanomater. Nanotechno.*, 27 (2015) 042001.
9. J. Wang, Z. C. Wu, H. B. Yin, W. Li and Y. Jiang, *RSC Adv.*, 4 (2014) 56926.
10. H. M. Ji, C. Liu, T. Wang, J. Chen, Z. N. Mao, J. Zhao, W. H. Hou and G. Yang, *Small*, 11 (2015) 6480.
11. W. Q. Zhou, X. M. Ma, F. X. Jiang, D. H. Zhu, J. K. Xu, B. Y. Lu and C. C. Liu, *Electrochim. Acta*, 138 (2014) 270.
12. P. Simon and Y. Gogotsi, *Nat. Mater.*, 7 (2008) 845-854.
13. D. Aradilla, F. Estrany and C. Alemán, *J. Phys. Chem. C*, 115 (2011) 8430.
14. P. Y. Tang, Y.Q. Zhao and C. L. Xu, *Electrochim. Acta*, 89 (2013) 300.
15. W. Lan, G. M. Tang, Y. R. Sun, Y. P. Wei, P. Q. La, Q. Su and E. Q. Xie, *J. Mater. Sci.: Mater. Electro.*, 27 (2015) 2741.
16. D. Shin, Y. Ko and J. Cho, *RSC Adv.*, 6 (2016) 21844.
17. F. X. Xiao, M. Pagliaro, Y. J. Xu and B. Liu, *Chem. Soc. Rev.*, 45 (2016) 3088.
18. Z. S. Wu, K. Parvez, S. Li, S. Yang, Z. Y. Liu, S. H. Liu, X. L. Feng and K. Mullen, *Adv. Mater.*, 27(2015) 4054-4061
19. A. K. Sarker and J. D. Hong, *Langmuir*, 28 (2012) 12637.
20. D. Aradilla, M. M. Pérez-Madrigal, F. Estrany, D. Azambuja, J. I. Iribarren and C. Alemán, *Org.*

- Electron.*, 14 (2013) 1483.
21. F. Estrany, D. Aradilla, R. Oliver, E. Armelin and C. Alemán, *Eur. Polym. J.*, 44 (2008) 1323.
 22. G. A. Snook, P. Kao and A. S. Best, *J. Power Sources*, 196B (2011) 1.
 23. Heywang G and J. F., *Adv. Mater.*, 4 (1992) 116.
 24. R. Liu, S. I. Cho and S. B. Lee, *Nanotechnology*, 19 (2008) 215710.
 25. Y. B. Xie, H. X. Du and C. Xia, *Micropor. Mesoporo. Mat.*, 204 (2015) 163.
 26. L. Tong, K. H. Skorenko, A. C. Faucett, S. M. Boyer, J. Liu, J. M. Mativetsky, W. E. Bernier and W. E. Jones, *J. Power Sources*, 297 (2015) 195.
 27. B. Anothumakkool, R. Soni, S.N. Bhange and S. Kurungot, *Energy Environ. Sci.*, 8 (2015) 1339.
 28. S. R. Sivakkumar, N. Angulakshmi and R. Saraswathi, *J. Appl. Polym. Sci.*, 98 (2005) 917.
 29. M. E. Plonska-Brzezinska, M. Lewandowski, M. Błaszcyk, A. Molina-Ontoria, T. Luciński and L. Echevoyen, *ChemPhysChem.*, 13 (2012) 4134.
 30. M. D. Stoller and R.S. Ruoff, *Energ. Environ. Sci.*, 3 (2010) 1294.
 31. Q. Wu, Y. X. Xu, Z. Y. Yao, A. R. Liu and G.Q. Shi, *ACS Nano.*, 4 (2010) 1963.
 32. J. Wang, Y. Xu, X. Chen, X. Du, *J. Power Sources*, 163 (2007) 1120-1125.
 33. X. M. Ma, D. H. Zhu, D. Z Mo, J. Hou, J. K. Xu, W. Q. Zhou, *Int. J. Electrochem. Sci.*, 10 (2015) 7941-7954.
 34. A.Q. Zhang, Y. Zhang, L.Z. Wang, X.F. Li, *Polym. Composite*, 32 (2011) 1-5.
 35. Y. G.Wang, Y. F. Song and Y. Y. Xia, *Chem. Soc. Rev.*, 45 (2016) 5925.
 36. D. Z. Mo, W. Q. Zhou, X. M. Ma and J. K. Xu, *Electrochim. Acta*, 155 (2015) 29.

© 2017 The Authors. Published by ESG (www.electrochemsci.org). This article is an open access article distributed under the terms and conditions of the Creative Commons Attribution license (<http://creativecommons.org/licenses/by/4.0/>).